Journal of Materials Chemistry B

Accepted Manuscript

ROYAL SOCIETY OF CHEMISTRY

www.rsc.org/materialsB

Journal of Materials Chemistry B

www.rsc.org/MaterialsB

PAPER

Preparation of novel magnetic cellulose nanocrystal and its efficient use for enzyme immobilization

Shi-lin Cao [a,b], Xue-Hui Li [a], Wen-Yong Lou [b,c*] and Min-Hua Zong [a,c*]

A novel biocompatible magnetic cellulose nanocrystals (MCNCs) composite was *in situ* prepared via a simple co-precipitation-electrostatic-self-assembly technique and was structurally characterized. Results showed that the anionic cellulose nanocrystals (CNCs) were successfully composited with cationic chitosan-coated Fe_3O_4 by self-assembly technology. The electrostatic interaction between CNCs and chitosan, and that between chitosan and Fe_3O_4, were the key driving forces for the formation of the composite. Papain, a widely used protease, could be successfully immobilized on the activated MCNCs with formaldehyde. The immobilized papain exhibited higher thermal stability than free enzyme, with the relative activity being higher than 80% after incubation at 40 °C for 7 h while that of free papain was less than 30%. Also, the pH stability of immobilized papain was superior to that of free papain. Moreover, the immobilized papain showed significantly better tolerance to the six solvents tested comparing with its free counterpart. The optimum range of pH for immobilized papain (pH 5 - 10) was remarkably wider than that of free enzyme (pH 5 - 7). The relative activities of immobilized papain at 50 - 70 °C were more than 90%, which significantly surpassed those of free papain. The immobilized papain also manifested excellent storage stability, with relative activity being as high as 93.6% after 16 days of storage at 4 °C. Furthermore, the obtained kinetic constant values showed that papain immobilized on the MCNCs had relatively high catalytic efficiency. Additionally, the immobilized papain could be easily separated and recycled from the reaction system through magnetic forces. Obviously, the prepared MCNCs as novel supports are promising and competitive for enzyme immobilization.

1 Introduction

Bio-based nanocomposites, manufactured via incorporating inorganic and/or natural organic nanomaterial into a natural polymer matrix, have gained more and more attention in this decade because of their eco-friendly properties [1].

Cellulose is the most abundant natural polymer on the earth. Cellulose nanocrystals (CNCs) are extracted from several kinds of cellulose, such as ramie, bacterial cellulose, cotton, microcrystalline cellulose, as well as waste cotton fabrics [2]. For preparing CNCs, raw materials are hydrolyzed with acid, usually sulfuric acid and hydrochloric acid. Depending on the crude material and isolation process, the length of the prepared CNCs ranged from approximately 20 nanometers to thousands of nanometers, while the reported width of CNCs was generally less than tens of nanometers and the aspect ratio (length-to-width) varied between 10 and 70 [3]. In recent years, CNCs have gained increasing attention in the nanomaterial field because of their excellent properties, including high surface-to-volume ratio, high aspect ratio, high stiffness, good hardness and strength. However, only limited number of studies that focused on CNCs as carriers of enzymes including glucose oxidase [4], peroxidase[5], and lysozyme [6] have been reported, where the incorporation of these enzymes conjugated onto the surface of CNCs gave significantly enhanced activity and stability and thus the catalytic efficiency. Obviously, the novel CNCs showed great potential applications for enzyme immobilization and was worthy of further study.

Nevertheless, the stable dispersion of the CNCs makes them difficult to recycle from the reaction system, thus limiting their applications. The mixture of magnetic nanoparticles (NPs) into the CNCs matrix is a feasible solution to the above problem. The utilization of magnetic NPs as enzyme carriers has recently attracted more and more attention, in that they not only greatly increased the stability of enzyme but also efficiently facilitated the recycle of enzymes from the reaction system [7-9]. In previous reports, the main approaches for preparing magnetic cellulose composites (not in nanoscale) were '*in situ*' synthesis [10] and the 'lumen-loading' process[11-12], which may not work on CNCs. The '*in situ*' method depends on the direct formation of ferrites and their loading on cellulose. Magnetic cellulose prepared by this method still suffered from the instability and the unsatisfactory loading amount of the magnetic composite. On the other hand, the 'lumen-loading' process relies on the deposition of magnetic pigment in the lumen of the fiber. However, it is difficult for the magnetic cellulose prepared with the method to improve the retention of inorganic particles and the mechanical strength of the cellulose fibers [13]. The naked-Fe_3O_4 directly deposited onto CNCs was unstable and readily leaked out from the surface of CNCs, mainly because both Fe_3O_4 and CNCs carried negative surface charge, giving rise to the charge repulsion with each other. Thus, it is particularly urgent to develop a new technique for preparation of the magnetic CNCs. Using biocompatible materials carrying positive surface charge such as chitosan could strongly combine Fe_3O_4 with CNCs via electrostatic self-

assembly and form stable magnetic CNCs, which might be of great potential for the preparation of immobilized enzyme.

Chitosan, the second most abundant natural polymer, is a biocompatible natural hydrophilic cationic polysaccharide (pK_a 6.3-7.0) due to the protonation of its $–NH_2$ group [14]. During the last five years, the study of chitosan-coated magnetic NPs has become a highly novel and promising research field [15], due to the outstanding performance of this kind of material in enzyme immobilization[16] and biomedicine[17]. It is noteworthy that chitosan and CNCs can combine with each other to form a biodegradable nanocomposite via electrostatic self-assembly and the electrostatic interactions between the negative charge on the CNCs and the positive charge on the chitosan are the driving forces for the preparation of these nanocomposites[1]. Thus, it's interesting to explore whether the magnetic NPs coated with chitosan combine with CNCs to form stable magnetic CNCs. The surface of NPs coated by chitosan carries positive charges and thus can electrically interact with the materials that carry negative surface charges [1]. Combining the magnetic NPs with CNCs using chitosan as an adhesion agent has several advantages: (1) enhancing the stability of the magnetic cellulose nanocrystals; (2) improving the biocompatibility of the material by utilizing cellulose and chitosan; (3) being inexpensive and eco-friendly.

In the present study, we, for the first time, have described the preparation of novel magnetic cellulose nanocrystals (MCNCs) as enzyme carriers using chitosan to strongly combine anionic CNCs with Fe_3O_4 through the simple co-precipitation-electrostatic-self-assembly technique. The electrostatic interaction between the CNCs and chitosan, and that between chitosan and Fe_3O_4 were found to be the key driving forces for the homogeneous and tight combination of the raw materials. The prepared biocompatible MCNCs were also successfully used as the supports for immobilization of papain that has wide applications in the fields of food, medicine and chemicals [18-20]. Furthermore, a comparative study has been made of MCNCs-based immobilized papain and free enzyme, and the obtained results showed that the novel MCNCs had tremendous potential for enzyme immobilization.

2 Experimental section

2.1 Materials

Materials. Cellulose microcrystalline was purchased from Sinopharm Chemical Reagent Co. Ltd. Hydrochloric acid (analytical grade, 36.5−38.0%) was from Guangzhou Chemical Reagent Co. Ltd. Papain from *Papaya latex* (rude powder 1.8 U/mg solid) was purchased from Sigma-Aldrich (USA). All other reagents were analytical reagents and obtained from commercial sources.

Apparatus. The FTIR analysis was carried out using a Tensor 37 spectrometer (Bruker, Germany) equipped with a deuterated triglycine sulfate (DTGS) detector. The spectra, acquired at a resolution of 4 cm^{-1} in the range of 400–4000 cm^{-1}, were the averages of 64 scans and were recorded against an empty cell as the background. Powder X-Ray Diffraction (XRD) was performed with a Bruker D8 Advance X-ray diffractometer with Ni-filtered Cu Ka radiation (k1 = 1.54 Å) generated at a voltage of 40 keV and a current of 40 mA was utilized. The scanning was performed from 4 to 60 ^{o} at a speed of 2^o min^{-1}. The crystallinity index (CI) values were calculated using the method described by Segal [21]. Magnetism measurements of the MCNCs were carried out at RT range from -20000Oe to 20000Oe by a vibrating sample magnetometer (VSM) option of the Physical Property Measurement System (PPMS-9, Quantum Design). Morphology of the materials was investigated via an EVO18 SEM (ZEISS, Germany) equipped with an energy dispersive spectrometer (EDS) operated at 10.0 kV. The samples were demagnetized and then sputter-coated with a thin overlayer of gold to prevent sample-charging effects before examination in the microscope. Zeta potential and size distribution of the samples were measured by Mastersize 2000 (Malvern Instrument).

2.2 Preparation of CNCs

The procedure for the preparation of CNCs is based on hydrochloric acid hydrolysis [22] with some modifications. In a typical experiment, 10 g of microcrystalline cellulose was mixed with 250 ml of 6 M HCl solution and subsequently heated at 90 ^{o}C under continuous stirring. After hydrolysis for 90 min, the suspension was cooled in a 4 ^{o}C water bath to stop the reaction and then washed with deionized water, followed by centrifugation at 4000 rpm for 5 min to remove the acid (repeated for 5 cycles) and then was dialyzed using regenerated cellulose dialysis membranes with 12–14 kDa molecular weight cut off and against deionized water until neutral pH was reached. Finally, the CNCs were dispersed in distilled water under stirring and the stock suspension of CNCs with a solid content of 6% was obtained.

2.3 Preparation of MCNCs

The preparation conditions are shown in **Table S1**. The MCNCs were prepared by self-assembly of CNCs with chitosan-coated Fe_3O_4. 6 g of the CNCs were dispersed in 100 ml distilled water and then mixed with 100 ml aqueous solution containing a given amount of $FeCl_2$•$4H_2O$ (1.34 - 5.36 g) and $FeCl_3$•$6H_2O$ (3.4 -13.6 g) (**Table S1**) , and then a 30 ml of 1% acetic acid buffer solution (pH 4.2) with chitosan (0.15 - 2.4 g) was added to the suspensions and the mixture was stirred for 60 min. Sodium tripolyphosphate (TPP, 0.3 – 4.8 g) suspension and 28% NH_4OH solution (20 ml) were added to the solution using a constant pressure funnel under slow stirring. The color of the suspension immediately turned black, demonstrating the formation of magnetite. The resulting solution was stirred for an additional 40 min at 80 ^{o}C. Subsequently, the resulting MCNCs were washed with deionized water and separated by centrifugation repeatedly for five times and stored as the stock suspensions with a solid content of 5 % by weight.

2.4 Immobilization of papain on the activated MCNCs

Before immobilization, the MCNCs were activated with formaldehyde. 10 g of the MCNCs suspensions (0.5 g solid) were centrifuged at 8000 rpm for 10 min to remove moisture. The remaining wet cake was dispersed in 10 ml 0.5% formaldehyde aqueous solution and then incubated for 1 h. After incubation, the MCNCs were washed with distilled water twice, for the removal of un-reacted formaldehyde and then stored in buffer solution for further use. For papain immobilization, the activated MCNCs

were incubated with a given concentrations of papain at 4 °C overnight. The uncross-linked papain was removed by washing with distilled water until no protein was detected by Bradford method [23]. These scrubbing solutions were combined to detect the amount of the uncross-linked papain. The amount of immobilized papain loading on the MCNCs could be calculated as the difference between the amount of the initial and the un-crosslinked papain.

2.5 Activity assay of free or immobilized papain

Chinese National Standard (GB/T 23527-2009) with slight modification was used for the determination of the activity of papain: a given amount of free papain or immobilized papain was dispersed in 2 ml buffer solution and subsequently mixed with 2 ml of 1% casein solution and incubated for 15 min at 60 °C. Subsequently, trichloroacetic acid solution was added to terminate the enzymatic reaction and the free amino acid was detected at 275 nm.

The activity of the free enzyme or the apparent activity of the immobilized enzyme (U/g enzyme) was defined as the amount of the formed tyrosine (μg) with 1 g of papain per min. The activity recovery of the immobilized enzyme was calculated as the ratio of immobilized papain activity to that of free papain of the same amount.

In order to study the optimal pH and temperature of both free and immobilized papains, the activities were measured over the pH range from 5 to 10 and temperature range from 30 °C to 80 °C.

The Michaelis-Menten constant (K_m) and the maximum reaction rate (V_{max}) of both free and immobilized enzymes, as well as the reusability of the immobilized papain, were detected as described previously [24]. For assaying the kinetic parameters of free and immobilized papains, the enzymatic hydrolysis of casein was used as the model reaction. The initial reaction rates were determined under the optimum reaction conditions (0.45 mg enzyme/ml, 60 °C, pH 6.5 for free enzyme or pH 7.0 for immobilized enzyme). The substrate concentrations varied from 1 to 15 mg/ml (0.1-1.5 wt %). Michaelis-Menten equation was used to fit the data (initial reaction rate vs. substrate concentration), and the kinetic parameters (K_m and V_{max}) of casein hydrolysis with free or immobilized papain were obtained from the fit.

For determining the pH stability and the thermo-stability of the enzyme, papain-immobilized-MCNCs containing 0.3 mg papain or 0.3 mg free papain were incubated in phosphate buffer (200 mM) with different pH values (5 - 9, at 40 °C) and various temperatures (40 - 80 °C, pH 7) for 1 - 7 h, and the residual activity was determined as above.

To learn organic solvent tolerance of the enzyme, papain-immobilized-MCNCs containing 0.3 mg papain or 0.3 mg of free papain were incubated in 0.15 mL n-butyl alcohol, $[Py_{14}]NTf_2$, or $[Emin]BF_4$ at 30 °C for 2 h and the residual activity of the enzyme was assayed.

All data reported were averages of experiments performed at least in triplicate, with no more that 2.0% standard deviation.

3. Result and discussion

3.1 Characteristic analysis of MCNCs

The FTIR spectra displayed in **Fig. 1** were recorded to confirm the chemical composition of the nanocomposite. The peaks at 1659 and 1599 cm^{-1} in **Fig. 1B** represented the amide I and Ⅱ groups of the chitosan, respectively [25]. The vibrational frequencies at 1165 and 1114 cm^{-1} were attributable to C-O-C and an asymmetrical ring, while the absorption peaks at about 667 and 613 cm^{-1} due to C-C-O and C-OH, respectively, were peaks of CNCs [26] (**Fig. 1C-1G**). Bending signals at 613 cm^{-1} were a typical frequency of beta-glycosilic linkages of sugar units. It was noteworthy that in the MCNCs spectra, the bands at 1599 cm^{-1} became weaker, which might be mainly caused by the strong hydrogen bonding between CNCs and chitosan and between chitosan and Fe_3O_4 [15]. Moreover, the chitosan characteristic peak of ($CONH_2$) at 1659 cm^{-1} shifted to 1639 cm^{-1} (a superposition with bending of the –OH of CNCs) and a considerably weak peak appeared at about 1510-1535 cm^{-1} (**Fig. 1E**), indicating that the tripolyphosphoric groups were successfully cross-linked with the ammonium group of chitosan via electrostatic interactions and the inter- and intramolecular interactions were enhanced in the chitosan matrix, as described previously [27-28]. The absorption at about 1165 cm^{-1} in the spectra of CNCs and the absorption at 1158 cm^{-1} for chitosan (**Fig. 1B**), which was assigned to the C–O–C stretch vibration, shifted to 1162 cm^{-1} in the MCNC spectra (**Fig. 1E**), demonstrating that the CNCs interacted with both chitosan and Fe_3O_4.

The diffractions from microcrystalline cellulose, CNCs (**Fig. 2C**) and MCNCs (**Fig. 2B**) could be resolved into peaks at 14.8°, 16.5°, 22.7°, and 34.5° , and they were assigned to the crystallographic planes of (101), (10-1), (002), and (040) [29], respectively; among these, the (101) and (002) lattice planes were identified as the amorphous and crystalline zone diffractions, respectively. These results indicated that the crystalline structure of cellulose was maintained during both acid hydrolysis and in-situ co-precipitation-self-assembly processes. Moreover, the crystallinity index (CI) values of microcrystalline cellulose was 60.30%, while that of CNCs was 69.83%, indicating that the acid cleavage preferentially occurred in disordered or paracrystalline regions of cellulose [30]. The high degree of crystallinity of chitosan was illustrated by the two strong peaks at 10.5° and 20.2°, as in a previous study [28]. However, with respect to the diffraction of the MCNCs, the characteristic peak of the chitosan (10.5°) vanished, demonstrating the chitosan formed a dense and disarrayed network structure of interpenetrating polysaccharides cross-linked with each other by poly-anion TPP [31]. The strong and distinct diffraction peak of magnetic Fe_3O_4 was recorded for MCNC-5 (**Fig. 2I**) and this confirmed the presence of the magnetic Fe_3O_4 (JCPDS card No. 19–0629) with the peaks at 2θ=18.31° (111), 30.04° (220), 35.58° (311), 43.19° (400), 53.63° (422), and 57.00° (511). However, the weak characteristic peaks of Fe_3O_4 could be seen at MCNC-4 (Fig. 2h) around 2θ = 18.2-18.5°(111), 30-31° (220), 35-36°(311), 43-43.5°(400), 53-53.5°(422), 57°(511). Moreover, because of the decrease of the ferric and chitosan contents of the MCNCs(**Fig. 2E-G**), the intensities of the Fe_3O_4 diffraction peak became weaker or disappeared, implying that the Fe_3O_4 particles were well encapsulated by the chitosan matrix, which inhibited the grain size of the crystalline Fe_3O_4 [32].

The saturated magnetizations, as measured by a vibrating magnetometer, were presented in **Table S2**. The highest saturated

magnetizations of the MCNCs were seen at MCNC-5 with the number 16.7249 emu/g. According to previous studies, saturated magnetization was significantly affected by the mass fraction of the magnetic iron oxides and the quenching of surface moments caused by the chitosan coating layer outside the Fe_3O_4 [33]. The magnetic properties of the MCNCs were consistent with the XRD results. As shown by **Fig. 3**, MCNC-5 could easily be attracted by an external magnetic field.

The zeta potentials of the samples were utilized to characterize the surface charge densities of the materials. **Fig. 4** showed the zeta potentials of chitosan, naked Fe_3O_4, CNC and magnetic CNC at different pH values. Both chitosan and CNCs carried like charges at pH range from both 1 to 3 and 8 to 10, indicating that these two polysaccharides repelled each other in these two pH ranges. Remarkably, chitosan and CNCs carried opposite surface charges at the pH range from 4 to 7 and in this range electrostatic attraction occurred. In a previous report, multilayered chitosan/CNC films were prepared via electrostatic layer-by-layer self-assembly due to the electrostatic interactions between negatively charged CNCs and positively charged chitosan [1]. On the other hand, naked-Fe_3O_4 carried a negative charge because of the abundant hydroxyl groups on the surface of the iron oxide, and hence it could be coated with chitosan molecules via self-assembly induced by electrostatic interactions, as described by Unsoy [17].

As evident from the SEM micrographs of the CNCs and the MCNCs in **Fig. 5A** and **Fig. 5B**, the aggregation of the prepared CNCs was observed upon freeze drying, forming fibrillar ribbons and dense block structures, which were very similar to the observations by Edwards [6]. The prepared CNCs and MCNCs had rodlike structures with the width of approximate 50 nm and the length of around 1000 nm. The CNCs are defined as the whisker-like materials with 3-100 nm width and 25-3000 nm length, and the sizes of the CNCs depend on the types of the used raw materials and the preparation conditions (Habibi et al., 2010). Thus, the synthesized materials in this article followed the definition of cellulose nanocrystals materials as well as the definition of nanomaterials. The micrographs of the SEM examination together with EDS mapping for the elements C, Fe, P and O were shown in **Fig. 5 C-H**. The bright regions indicated the presence of elements C, Fe and O, demonstrating that the iron oxide was distributed uniformly on the surfaced of the CNCs throughout the entire area.

It is of great interest to know the size and distribution of the Fe_3O_4 NPs coated with chitosan on the surface of CNCs. The TEM analysis of the prepared MCNCs as well as Fe_3O_4 NPs coated with chitosan (magnetic NPs prepared without CNCs) was carried out. As can be seen in **Fig. S1**, the Fe_3O_4 NPs coated with chitosan were dispersed stably and homogeneously on the surface of CNCs. The size of Fe_3O_4 NPs coated with chitosan was shown to be 10-20 nm. Furthermore, the magnetic NPs prepared in the absence of CNCs have the same size of 10-20 nm, suggesting that the CNCs didn't significantly affect the size of Fe_3O_4 NPs coated with chitosan bound on the surface of the CNCs.

As depicted in **Fig. 6**, the MCNCs were prepared *in situ* by simple co-precipitation-electrostatic-self-assembly technique. Initially, both Fe^{2+} and Fe^{3+} ions can be chelated by the amino groups ($-NH_2$) of chitosan [34], and formed a stable complex of Fe^{2+} and Fe^{3+} ions wrapped with chitosan. Subsequently, chitosan bearing Fe^{2+} and Fe^{3+} ions cross-linked in the presence of TPP through electrostatic interactions between positively charged groups of chitosan and negatively charged groups of TPP, and formed a complex with a dense and disarray chitosan network, limiting the growth of the iron oxide core and thus yielding smaller particles [35] in the following process. After NH_4OH was added into the mixture, Fe_3O_4 NPs were then formed and coated by chitosan molecules. When the pH of the mixture decreased to around 7.0, the surface of chitosan carried positive charges and that of CNCs carried negative charges, thus resulting in the binding of Fe_3O_4 NPs coated with chitosan to CNCs via electrostatic self-assembly and forming the MCNCs.

3.2 Characteristics of free and immobilized enzymes

The amide I had absorption bands ranging from 1600 to 1700 cm^{-1}, attributed to the C=O stretching, while the amide II bands (due to C - N stretching and NH bending) were at about 1550 cm^{-1} [36]. **Fig. 7** revealed the FTIR spectra of free and immobilized papain. The spectrum of both immobilized and free enzymes had similar amide bands for amide I and II. However, the bands of the immobilized enzyme were less intense compared with the free papain, indicating that the papain had been successfully attached onto the MCNCs support, and retained its typical bonds [37]. The activity recovery of papain significantly decreased with increasing amount of protein loading in the support materials, as indicated by the observation that the activity recovery of enzyme reduced from around 99% to 44% with the increase of the protein loading amount from 2.2 to 14.5 mg/g. The apparent activity of papain immobilized on the MCNCs was around 1832.3 U/g support with the protein loading of 8.9 mg enzyme/ g support, and consequently the specific activity of immobilized papain was calculated to be 205.9 U/mg proteins. The specific activity of free papain was detected to be about 276.5 U/mg proteins. Therefore, the activity recovery of papain was shown to be 74.5%. Papain is usually used for proteolysis (macromolecular substrates), excessive enzyme loading on the support will cause internal mass-transfer limitations, which leading to a decrease in the specific activity and activity recovery of the immobilized papain[38]. Thus, the amount of papain loading on the surface of the MCNCs (8.9 mg enzyme / g support) is suitable for macromolecular substrates proteolysis. Additionally, the activity of papain immobilized on Fe_3O_4 NPs wrapped with chitosan (magnetic NPs prepared without CNCs) was determined and compared with that of papain immobilized on the MCNCs. It was found that the apparent activity of papain immobilized on Fe_3O_4 NPs coated with chitosan was about 1534.6 U/g support with the protein loading of around 8.3 mg enzyme/ g support and the activity recovery was 66.5%. As a result, the specific activity of papain immobilized on Fe_3O_4 NPs coated with chitosan was estimated to be 183.9 U/mg proteins. Clearly, the activity of MCNCs-based immobilized papain was superior to that of papain immobilized on Fe_3O_4 NPs coated with chitosan. In comparison with Fe_3O_4 NPs coated with chitosan, the MCNCs gave relatively higher protein loading and specific activity, which might be attributable to the abundant active -OH groups of the CNCs [39] that contribute to the cross-linking of papain onto the MCNCs. On the other hand, it is of great interest to explore the

biocompatibility of the prepared MCNCs support with papain. From the data summarized in Table S3, papain maintained more than 96% of its initial activity even after being incubated with a relatively high amount of the MCNCs (150 mg) for 1 h, indicating the good biocompatibility and great potential as the support for enzyme immobilization, of the novel material MCNCs .

The effect of the electrostatic interaction on the immobilization efficiency of papain was also investigated. The surface charge of papain was measured at a pH range of 2-10 and the loading amount of the enzyme on the MCNCs via electrostatic interaction in the absence of formaldehyde were examined (Fig. S2). It was found that the change of pH significantly affected the surface charges of papain and MCNCs and thus the enzyme loading on the MCNCs by electrostatic interaction. However, the loading amount of the enzyme on the MCNCs by electrostatic interaction at different pHs was less than 0.9 mg enzyme/ g support, which was much lower than that of the enzyme immobilized on the MCNCs by cross-linking (8.9 mg enzyme/g support), demonstrating that papain was immobilized on the MCNCs mainly by cross-linking with formaldehyde.

The effect of pH on free or immobilized papain was studied in the pH range of 5 to 10. As shown in Fig. 8, the maximum activities of the free and immobilized papain were observed at pH 6 and 7, respectively, illustrating that the optimum medium pH value of immobilized papain shifted in the alkaline direction. Additionally, the leaching of papain from the MCNCs with pH change from 2 to 10 was examined, and no significant leakage of protein was found, showing that the change of papain's activity with pH (**Fig 8**) was not attributable to the leaching of protein from the support. The alkaline shift of the optimal pH of the immobilized papain might attribute to the interactions between the enzyme and the polymeric matrix, such as hydrogen bonding[24, 40-42] and electrostatic interactions [43-44]. It has been clearly demonstrated that the synthesized MCNCs' surface is positively charged, which could reduce the hydroxyl ion concentrations around the surface of the support and consequently the pH of the support surface will be lower than that of the bulk solution. Therefore, the optimal pH of papain immobilized on the MCNCs shifted to the alkaline direction, which is very similar to the observation by the pH shift for other enzymes immobilized on the supports carrying positive surface charges reported previously [43-44]. The immobilized papain exhibited a higher relative activity compared to free papain, especially at pH 10, where immobilized papain retained 61.7% of relative activity while the corresponding value for its free counterpart was about 40.3%. In general, the papain immobilized on the carriers exhibited good adaptability to pH, particularly to environmental alkalinity. These results were in accordance with a previous report [45].

As can be seen in **Fig. 9**, although the maximum activities were recorded at 60 ^{o}C for both immobilized and free enzymes, immobilized papain retained more than 92% of its relative activity at temperatures ranging from 50 to 70 ^{o}C, whereas the residual activity levels of the free papain at 50 and 70 ^{o}C were approximately 88.3 and 82.5%, respectively. Above 70 ^{o}C, the relative activity of free papain dropped sharply and it retained only 30.1% at 80 ^{o}C. In contrast, the immobilized papain remained about 66.0% of the relative activity. The good heat resistance might be due to the prevention of autolysis of the papain. Similar observation was also made by other research group[45].

In order to investigate the stability of the immobilized papain under different pH levels, the enzyme was incubated at 40 ^{o}C in phosphate buffer (50 mM, pHs 5 - 9) for 7 h (Fig. 10). The immobilized papain retained more than 64.5% of its initial activity, while the relative activity of the free enzyme was only around 26.2%, indicating that the immobilized enzyme had much higher pH stability. Moreover, it was found that papain was more stable under neutral and alkaline environments (pHs 7 - 9) than acidic conditions (pHs 5 - 6).

As illustrated in **Fig. 11**, the immobilized papain kept above 77.2% of its original activity after incubated for 7 h at 40 ^{o}C, whereas less than 30% of residual activity was detected with its free counterpart. The free papain retained about 12.1% residual activity after 1 h incubation at 80 ^{o}C, while about 65.6% of the residual activity was recorded with immobilized papain. The higher thermal stability of immobilized papain might be attributable to the stabilization of enzyme molecules by MCNCs [46].

As shown in **Fig. 12**, the immobilized papain exhibited significantly better tolerance to all three solvents tested comparing with its free counterpart. Among them, $[Py_{14}]NTf_2$ had the lowest toxicity to immobilized papain while *n*-butyl alcohol had lowest toxicity to free papain. It was worth noting that although both biocatalysts were significantly deactivated by $[Emin]BF_4$, the residual activity of immobilized papain was much higher than that of the free enzyme (55.52% *vs* 21.09%). Similarly, 2 h exposing to $[Py_{14}]NTf_2$ almost caused 48.15% loss of the activity of free papain, the immobilized papain retained 71.4% of its initial activity. Obviously, the MCNCs-immobilized biocatalyst showed higher resistance to inactivation comparing with the free counterpart in all these solvent systems. Generally, organic solvents or ionic liquids with relatively higher polarity could strip off the protein-bound water from the surface of enzyme and break the native structure of an enzyme[47], thus resulting in rapid deactivation of enzyme. In the case of papain immobilized on the MCNCs by cross-linking with formaldehyde, the enzyme exhibited more rigidity and could well maintain its catalytic conformation in the reaction system. Thus, papain manifested greatly enhanced tolerance to organic solvents and ionic liquids and retained relatively high catalytic activity even in polar solvents after immobilization, which was supported by previous reports[48-49].

To examine the storage stability of enzyme, both free and immobilized papains were stored at 4 ^{o}C in phosphate buffer. The immobilized papain showed superior retention of activity than free papain (**Fig. 13**). After 16 days of storage, the immobilized papain retained 93.6% of its initial activity while the corresponding value for its free counterpart was 44.5%. Obviously, the immobilized papain had better storage stability.

The kinetics behaviors of casein hydrolysis with free and immobilized papains were comparatively studied. It was found that the papain-mediated hydrolysis of casein followed Michaelis-Menten equation. The kinetic parameters K_m for free and immobilized papains were 13.5 and 10.0 mg/ml, respectively,

demonstrating the increase of the enzyme-substrate affinity of immobilized papain[50]. The V_{max} for immobilized papain was 6.5×10^{-2} mg/(ml•min), which was lower than that for free papain (8.4×10^{-2} mg/(ml•min)). This was in good agreement with the observation that the specific activity of immobilized papain was lower than that of free enzyme (205.9 *vs.* 276.5 U/mg). Additionally, the K_{cat}/K_m value of immobilized papain was higher than that of free papain (2.15×10^{-2} *vs* 2.07×10^{-2} mg/(ml•min)), indicating that the papain immobilized on this novel MCNCs had relatively high catalytic efficiency.

The immobilized papain retained more than 90% of its original catalytic activity after successive re-use of three cycles, and the relative activity was around 63% even after five cycles of re-use.

4. Conclusion

Novel biocompatible MCNCs were successfully prepared by a simple co-precipitation-electrostatic-self-assembly technique for the first time. The MCNCs proved to be potential carriers for enzyme immobilization and the papain immobilized on MCNCs had higher activity, improved pH, thermal and storage stabilities, and enhanced tolerance to organic solvents and ionic liquids than its free counterpart. The kinetic study for both immobilized and free enzyme showed that the papain immobilized on the novel MCNCs had relatively high catalytic efficiency.

Graphics

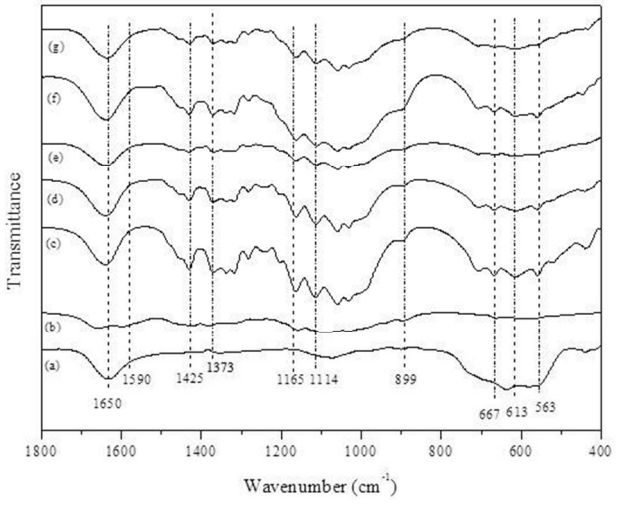

Fig.1 FTIR spectra for nake-Fe_3O_4 (a), chitosan (b), CNCs (c), MCNCs-1 (d), MCNCs-2 (e), MCNCs-3 (f), MCNCs-4 (g).

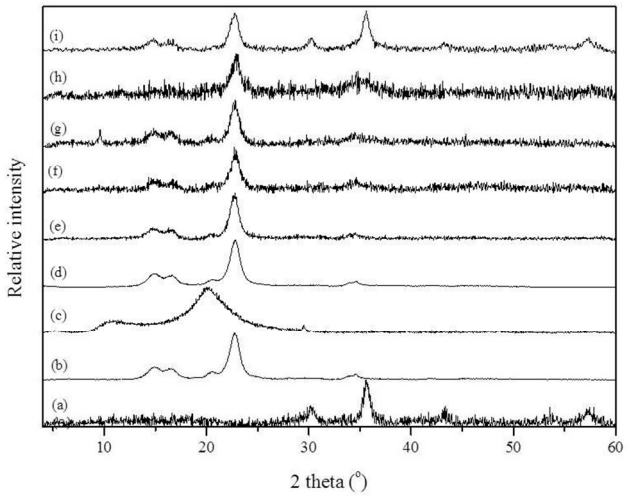

Fig.2 XRD Spectra for nake-Fe_3O_4 (a), MCC (b), chitosan (c), CNCs (d), MCNCs-1 (e), MCNCs-2 (f), MCNCs-3(g), MCNCs-4 (h), MCNCs-5 (i).

Fig.3 MCNCs-5 (left) dispersed in aqueous solution and MCNCs-5 attracted by external magnetic fields (right).

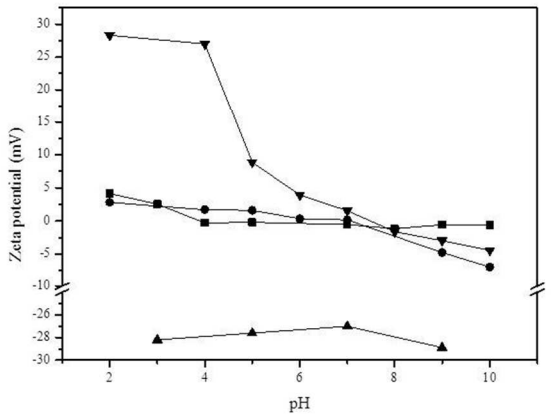

Fig4. Zeta potential at different pH of chitosan (▼), naked Fe_3O_4(▲), MCNC-1 (●) and CNCs (■)

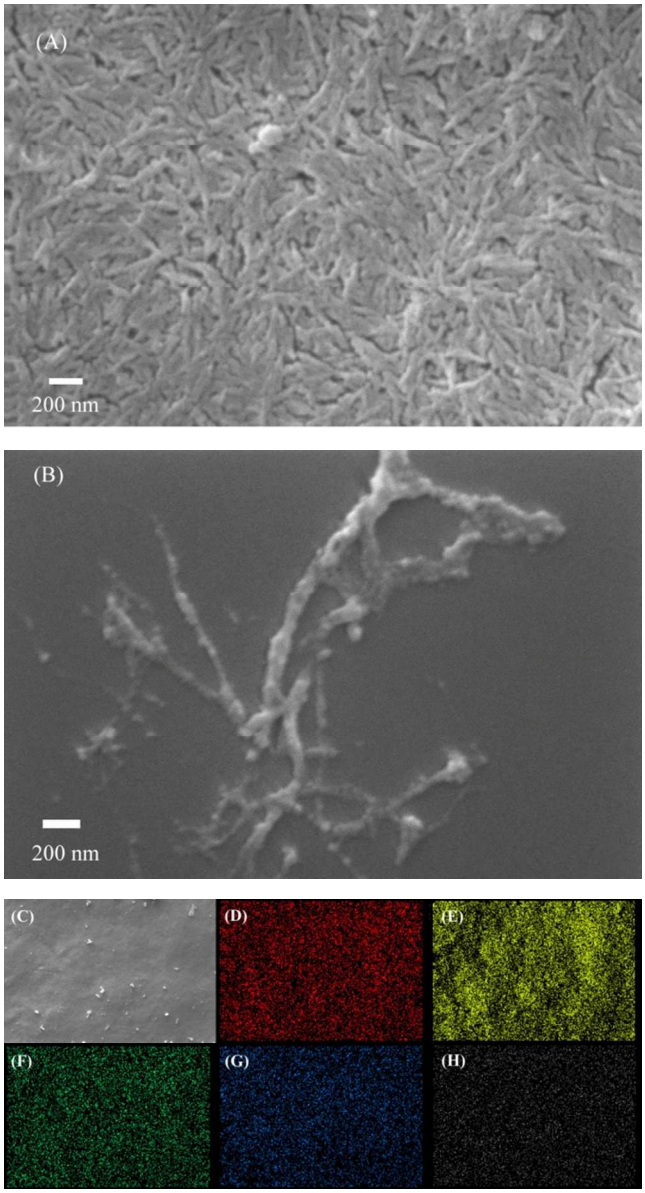

Fig.5 Scanning electron micrographs of (A) CNCs, (B) MCNCs, (C).MCNCs with corresponding EDS maps for elements (B) C, (C) O,(D) P, (E)Fe, (F) Au.

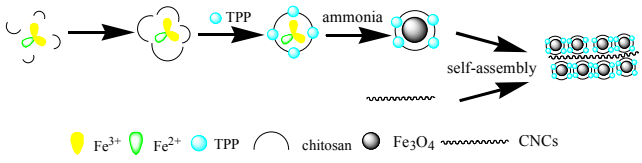

Fig.6 Schematic representation of experimental protocols for preparation of MCNCs.

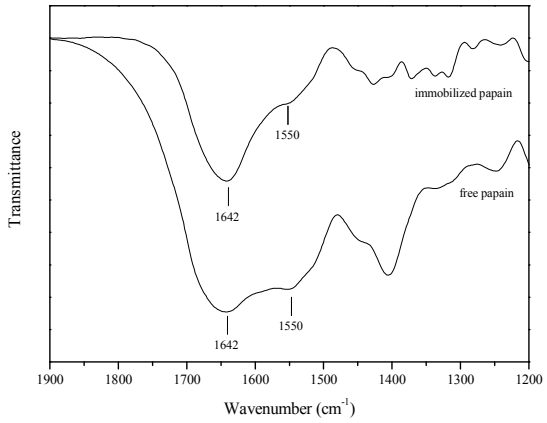

Fig.7 FTIR spectra for papain and immobilized papain.

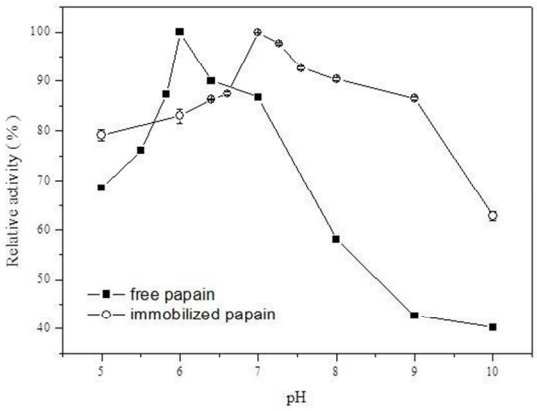

Fig.8 Effect of pH on the free papain (■) and immobilized papain (○).

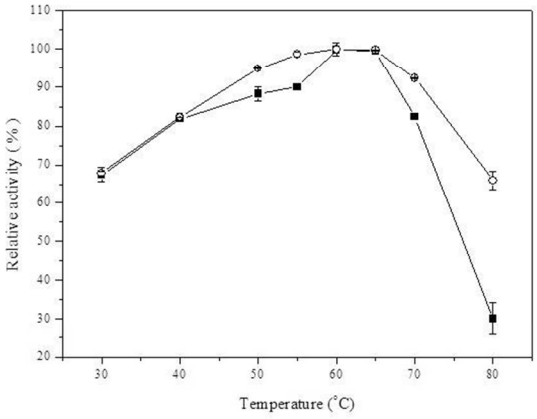

Fig.9 Effect of temperature on the free papain (■) and immobilized papain (○).

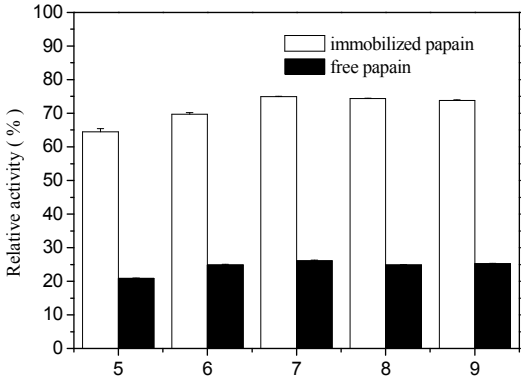

Fig.10 Effect of pH on the thermal stability of the free papain (Symbols: □) and immobilized papain (Symbols:■).

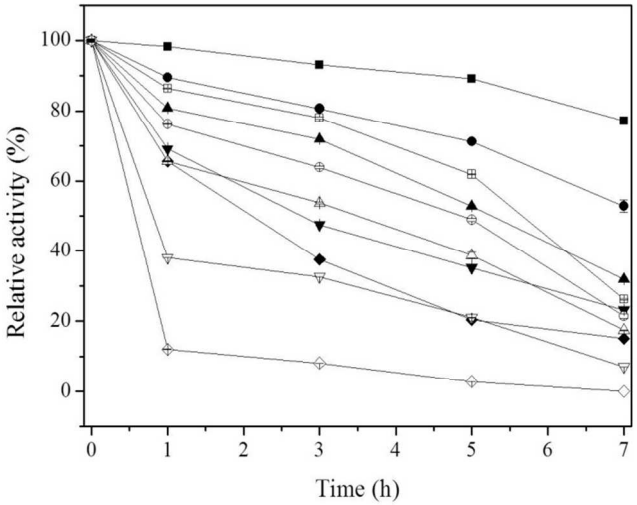

Fig.11 Thermal stability of the free papain (Symbols: 40 ºC (□); 50 ºC (○); 60 ºC(△) ;70 ºC (▽); 80 ºC (◇)) and immobilized papain (Symbols: 40 ºC (■); 50 ºC (●); 60 ºC(▲) ;70 ºC (▼); 80 ºC (♦)).

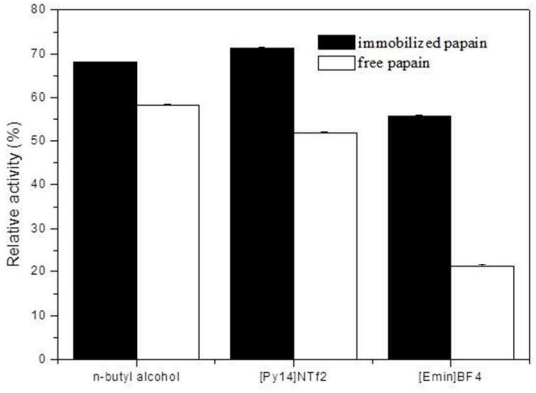

Fig.12 Organic solvent tolerance of the free papain (□) and immobilized papain (■).

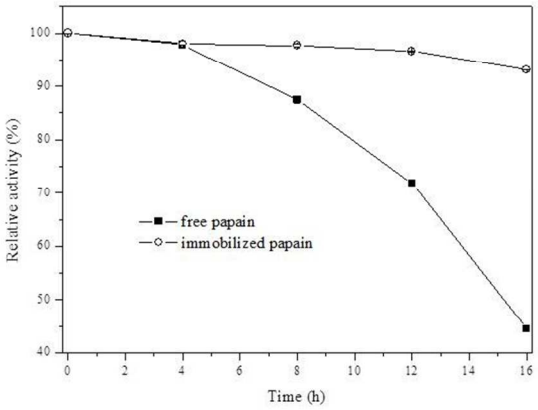

Fig.13 Storage stability of the free papain (■) and immobilized papain (○).

Acknowledgements

We wish to thank the National Science Found for Excellent Young Scholars (21222606), the State Key Program of National Natural Science Foundation of China (21336002), the Key Program of Guangdong Natural Science Foundation (S2013020013049), the National Key Basic Research Program of China (2013CB733500) and the Fundamental Research Funds for SCUT (2013ZG0003) for partially funding this work. We also thank Dr. Hong Huang (Instrumental Analysis & Research Center, Sun Yat-Sen University, China) for TEM analysis.

Notes and references

[a] *School of Chemistry and Chemical Engineering, South China University of Technology, Guangzhou 510640, China.*
[b] *State Key Laboratory of Pulp and Paper Engineering, College of Light Industry and Food Sciences, South China University of Technology, Guangzhou 510640, China. Fax: 86-20-87111452; Tel: 86-20-87111452; E-mail: btmhzong@scut.edu.cn*
[c] *Lab of Applied Biocatalysis, South China University of Technology, Guangzhou 510640, China. Fax: 86-20-22236669; Tel: 86-20-22236669; E-mail: wylou@scut.edu.cn*

† Electronic Supplementary Information (ESI) available: see attachment.

1. J. P. de Mesquita, C. L. Donnici and F. V. Pereira, *Biomacromolecules*, 2010, **11**, 473-480.
2. R. Xiong, X. X. Zhang, D. Tian, Z. H. Zhou and C. H. Lu, *Cellulose*, 2012, **19**, 1189-1198.
3. Y. Habibi, L. A. Lucia and O. J. Rojas, *Chemical reviews*, 2010, **110**, 3479.
4. V. Incani, C. Danumah and Y. Boluk, *Cellulose*, 2013, **20**, 191-200.
5. F. W. a. S. W. R. Yang, *Biotechnology*, 2008, **7**, 233-241.
6. J. V. Edwards, N. T. Prevost, B. Condon, A. French and Q. Wu, *Cellulose*, 2012, **19**, 495-506.
7. N. A. Kalkan, S. Aksoy, E. A. Aksoy and N. Hasirci, *Journal of Applied Polymer Science*, 2012, **123**, 707-716.
8. J. Wang, G. Zhao, Y. Li, X. Liu and P. Hou, *Appl Microbiol Biotechnol*, 2013, **97**, 681-692.
9. X. Liu, X. Chen, Y. Li, X. Wang, X. Peng and W. Zhu, *ACS Applied Materials & Interfaces*, 2012, **4**, 5169-5178.

10. C. Chia, S. Zakaria, K. Nguyen and M. Abdullah, *Industrial Crops and Products*, 2008, **28**, 333-339.
11. S. Zakaria, B. Ong and T. Van de Ven, *Colloids and Surfaces A: Physicochemical and Engineering Aspects*, 2004, **251**, 1-4.
12. S. Zakaria, B. Ong and T. Van de Ven, *Colloids and Surfaces A: Physicochemical and Engineering Aspects*, 2004, **251**, 31-36.
13. J. Shen, Z. Song, X. Qian and Y. Ni, *Industrial & Engineering Chemistry Research*, 2010, **50**, 661-666.
14. P. Schulz, M. Rodriguez, L. Del Blanco, M. Pistonesi and E. Agullo, *Colloid and Polymer Science*, 1998, **276**, 1159-1165.
15. Z. Liu, H. Wang, B. Li, C. Liu, Y. Jiang, G. Yu and X. Mu, *Journal of Materials Chemistry*, 2012, **22**, 15085-15091.
16. Y. Wu, Y. Wang, G. Luo and Y. Dai, *Bioresource Technol*, 2009, **100**, 3459-3464.
17. G. Unsoy, S. Yalcin, R. Khodadust, G. Gunduz and U. Gunduz, *J Nanopart Res*, 2012, **14**, 1-13.
18. E. Amri and F. Mamboya, *American Journal of Biochemistry and Biotechnology*, 2012, **8**, 99-104.
19. W. Y. Lou, M. H. Zong, T. J. Smith, H. Wu and J. F. Wang, *Green Chem.*, 2006, **8**, 509-512.
20. X. Qin, W. Xie, Q. Su, W. Du and R. A. Gross, *Acs Catalysis*, 2011, **1**, 1022-1034.
21. L. Segal, J. Creely, A. Martin and C. Conrad, *Textile Research Journal*, 1959, **29**, 786-794.
22. B. Braun and J. R. Dorgan, *Biomacromolecules*, 2009, **10**, 334-341.
23. M. M. Bradford, *Analytical biochemistry*, 1976, **72**, 248-254.
24. G. Bayramoglu, B. F. Senkal, M. Yilmaz and M. Y. Arica, *Bioresource Technol*, 2011, **102**, 9833-9837.
25. J. Brugnerotto, J. Lizardi, F. M. Goycoolea, W. Arguelles-Monal, J. Desbrieres and M. Rinaudo, *Polymer*, 2001, **42**, 3569-3580.
26. A. C. Leung, S. Hrapovic, E. Lam, Y. Liu, K. B. Male, K. A. Mahmoud and J. H. Luong, *Small*, 2011, **7**, 302-305.
27. Y. Xu and Y. Du, *International Journal of Pharmaceutics*, 2003, **250**, 215-226.
28. L. Qi, Z. Xu, X. Jiang, C. Hu and X. Zou, *Carbohydrate Research*, 2004, **339**, 2693-2700.
29. H.-L. Chen and A. Yokochi, *Journal of Applied Polymer Science*, 2000, **76**, 1466-1471.
30. H. Kargarzadeh, I. Ahmad, I. Abdullah, A. Dufresne, S. Zainudin and R. Sheltami, *Cellulose*, 2012, **19**, 855-866.
31. E. S. K. Tang, M. Huang and L. Y. Lim, *International Journal of Pharmaceutics*, 2003, **265**, 103-114.
32. H. Liu, E. Jiang, H. Bai and R. Zheng, *Journal of applied physics*, 2004, **95**, 5661-5665.
33. H. Xu, N. Tong, L. Cui, Y. Lu and H. Gu, *Journal of magnetism and magnetic materials*, 2007, **311**, 125-130.
34. Y. Wang, B. Li, Y. Zhou and D. Jia, *Polymers for Advanced Technologies*, 2008, **19**, 1256-1261.
35. D. Hritcu, M. I. Popa, N. Popa, V. Badescu and V. Balan, *Turk J Chem*, 2009, **33**, 785-796.
36. M. Carbonaro and A. Nucara, *Amino acids*, 2010, **38**, 679-690.
37. A. V. Paula, D. Urioste, J. C. Santos and H. F. de Castro, *Journal of Chemical Technology and Biotechnology*, 2007, **82**, 281-288.
38. M. Wang, C. Jia, W. Qi, Q. Yu, X. Peng, R. Su and Z. He, *Bioresource Technol*, 2011, **102**, 3541-3545.
39. P. Tingaut, T. Zimmermann and G. Sèbe, *Journal of Materials Chemistry*, 2012, **22**, 20105-20111.
40. S. Akgöl, Y. Kacar, A. Denizli and M. Arıca, *Food Chem.*, 2001, **74**, 281-288.
41. Q. D. Nguyen, J. M. Rezessy-Szabó, B. Czukor and Á. Hoschke, *Process Biochem.*, 2011, **46**, 298-303.
42. J. Jordan, C. S. Kumar and C. Theegala, *J. Mol. Catal. B: Enzym.*, 2011, **68**, 139-146.
43. K. Sangeetha and T. E. Abraham, *J. Mol. Catal. B: Enzym.*, 2006, **38**, 171-177.
44. S. S. Khaparde and R. S. Singhal, *Bioresource Technol*, 2001, **78**, 1-4.
45. H. Lei, W. Wang, L. L. Chen, X. C. Li, B. Yi and L. Deng, *Enzyme and Microbial Technology*, 2004, **35**, 15-21.
46. K. A. Mahmoud, E. Lam, S. Hrapovic and J. H. T. Luong, *ACS Applied Materials & Interfaces*, 2013, **5**, 4978-4985.
47. C.-Y. Yu, X.-F. Li, W.-Y. Lou and M.-H. Zong, *J. Biotechnol.*, 2013, **166**, 12-19.
48. D. Susanti, T. Suhartati and S. Hadi, *Modern Applied Science*, 2012, **6**.
49. Z. Yang, M. Domach, R. Auger, F. X. Yang and A. J. Russell, *Enzyme and Microbial Technology*, 1996, **18**, 82-89.
50. H.-Y. Gu, A.-M. Yu and H.-Y. Chen, *Journal of Electroanalytical Chemistry*, 2001, **516**, 119-126.